Article:
Faik, A.M.E.D., Zhang, Y. and Hanriot, S.D.M. (2019) Droplet Combustion Characteristics of Biodiesel–Diesel Blends using High Speed Backlit and Schlieren Imaging. Heat Transfer Engineering, 40 (13-14). pp. 1085-1098. ISSN: 0145-7632

https://doi.org/10.1080/01457632.2018.1457209

Droplet Combustion Characteristics of Biodiesel–Diesel Blends using High Speed Backlit and Schlieren Imaging

Ahmad Muneer El-Deen Faik[1, 2], Yang Zhang[1], Sérgio de Morais Hanriot[3]

[1]Department of Mechanical Engineering, The University of Sheffield, UK

[2]Mechanical Engineering Department, Al-Mustansiryah University, Baghdad, Iraq

[3]Department of Mechanical Engineering, Pontifical Catholic University of Minas Gerais, Brazil

Address correspondence to Professor Yang Zhang, Department of Mechanical Engineering, The University of Sheffield, Sir Frederick Mappin Building, Mappin Street, Sheffield, S1 3JD, United Kingdom. E-mail: yz100@sheffield.ac.uk

Telephone: +44(0)114 2227880 Fax: +44(0)114 2227890

ABSTRACT

This work investigates the effect of blending biodiesel with diesel on the combustion of an isolated fuel droplet. Biodiesel blends substituting diesel oil in different concentrations on volumetric basis, in addition to neat diesel and biodiesel were studied. High speed schlieren and backlighting imaging techniques have been used to track droplet combustion. The results showed that partial substitution of diesel oil by biodiesel at the test conditions led to increasing secondary atomization from the droplet, compared to neat diesel or biodiesel fuel droplets. This in turn enhances evaporation, mixing, and then combustion. Additionally, the results showed that biodiesel has a higher burning rate compared to diesel, and that increasing biodiesel in the blend increases the burning rate of the blend. Nucleation has also been traced to take place inside the droplets of the blends. Moreover, flame size (height and width) has been reduced by increasing biodiesel concentration in the blend.

INTRODUCTION

Diesel fuels constitute the main source of pollutant emissions. Studies have shown that the formation of these pollutants can be reduced by including oxygenated fuels on diesel blends [1,2]. Biodiesels are presently the most widely attractive fuels for this objective due to various advantages; such as higher biodegradation, reduced toxicity, safe storage, and enhanced lubricity compared to the ordinary diesel fuels [3]. In fact, they are being increasingly utilized in gas turbine engines [4–6] in addition to the compression ignition engines [7–10]. Biodiesels are derived from animal fats or vegetable oils and are usually blended with diesel in different proportions and used without substantial engine modifications. This is due to the complete miscibility of biodiesel on diesel fuels [3]. However, compared to conventional diesel fuels, biodiesel has a higher viscosity that results in poor atomization characteristics [3,11], and a higher NOx emission due to the increase in combustion efficiency and adiabatic flame temperature by the presence of oxygen in biodiesel [8,12]. Therefore, biodiesel addition to diesel in the form of blends is practically advocated than complete replacement.

Consequently, liquid fuel spray is an integral of small size droplets [13]. Therefore, understanding droplet combustion gives a good insight towards the understanding of the combustion characteristics of the liquid fuel spray. Hence, droplet combustion of biodiesel-blended diesel has been a widely studied subject. A variety of biodiesel fuels according to production method and raw elements, in addition to variable blending ratios and variable droplet configurations (suspended and freely falling droplets) have been used for studying the combustion of biodiesel-blended diesel fuel droplet. Botero et al., [14] have studied the effect of blending diesel with castor oil biodiesel on the combustion of freely falling droplets. They observed a significant reduction of soot formation in the blends compared to diesel. And they

found that the burning of biodiesel is lower than that of diesel due to lower heating value and higher boiling point of bioethanol compared to diesel. Pan and coworkers used a freely falling chamber for studying the combustion of multicomponent fuel droplet consisting of diesel-biodiesel blends [15] and diesel-biodiesel-alcohol blends [16] under reduced gravity conditions. The droplet is suspended by a ceramic fiber inside the chamber. They pointed out the decrease in soot shell around the diesel droplet by biodiesel addition. Additionally, they showed that the biodiesel blends are generally following the characteristics of the multicomponent fuel droplet combustion. Li et al., [17] have studied the effect of blending diesel with fatty acid methyl ester (FAME) biodiesel on the combustion characteristics of a freely falling droplet. However, they claimed that biodiesel has a higher burning rate compared to diesel, which is controversial to the previous results. Whereas Zhu et al., [18] have found that blending diesel with methyl oleate (as biodiesel) results in decreasing the burning rate and flame temperature to certain levels for blends of less than 20% methyl oleate. Then, both are increased when increasing methyl oleate concentration in the blend. Xu et al., [19] studied the droplet combustion of algae-based biodiesel and its equi-volume blend with diesel (BD50). They found that the burning rate of both biodiesel and BD50 are close to that of the conventional diesel.

Broadly speaking, it can be inferred that there are different types of biodiesel fuels depending on the method and raw elements used for production. Each of these types has its own chemical and physical properties in addition to the variety of conventional diesel fuels. Therefore, a unified description of the combustion characteristics of diesel-biodiesel blends is hardly affordable. Hence, experimental investigation is desirable for studying the combustion characteristics of the resulting blends from any diesel-biodiesel combination. This in turn, is the first objective of the present work. On the other hand, it can be seen that the majority of the

conducted work is aimed to evaluating droplet size evolution, burning rate, and flame to droplet stand-off ratio, which are the basic investigated parameters. Though, there are some other parameters that are as important as the aforementioned ones. Secondary atomization is one of these parameters that are of practical importance in spray combustion systems due to its role in enhancing fuel-air mixing and then improving combustion efficiency. Secondary atomization is the processes of droplet disintegration into smaller size droplets. This disintegration results when the dynamic forces acting on the droplet are higher than the restoration force of the droplet [20]. Droplet dynamics during the combustion of multicomponent fuel droplets are of importance as well, since the combustion of these droplets is relatively different from that of a single component droplet. Therefore, the main objective of the current work is to give an insight full scale exploration of the combustion characteristics of the biodiesel-blended diesel fuel droplet using high speed imaging. This exploration is carried out using backlit imaging for droplet and flame size investigations, in addition to tracking secondary atomization using Schlieren imaging. Schlieren imaging gives the capability of differentiating between different objects by temperature gradient. Therefore, it is useful for tracking the small size sub-droplets emitted from the original droplet.

EXPERIMENTAL WORK

Biodiesel blends substituting diesel oil in concentrations of 7%, 10%, 20% and 30% on volumetric basis, in addition to neat diesel and neat biodiesel have been studied. For simplicity, the blends will be symbolized as BD07, BD10, BD20, and BD30, while diesel and biodiesel will be given the symbols D100 and B100 respectively. The biodiesel fuel used in experiments is a B100 Petrobras biodiesel; it is basically a Methyl ester derived from tallow and soybeans oil of

40% and 60% by volume respectively. The physical properties of both diesel and biodiesel are listed in Table 1. The diesel-biodiesel blends are prepared in lab prior to experiments. Fuel droplets are generated and suspended on a 75 µm cross-shaped silicon carbide (SiC) fibre mesh using a micro-fine syringe with hypodermic (0.33*12.7mm) needle. A relatively constant volume of fuel is injected by the syringe to minimize droplet size variation throughout the different tests. A Photron-SA4 high speed colour camera has been used for tracking droplet lifetime during combustion with two different techniques. The former is backlighting imaging which is used for tracking droplet and flame size evolution. In this technique, two 6-volt LED lights with white light diffuser have been mounted behind the droplet and opposite to the camera lens as shown in Figure 1. A Nikon AF Micro NIKKOR 60mm f/2.8D lens with a 55mm macro extension tube set is attached to the camera for obtaining a detailed focused image of the droplet and the corresponding flame. Camera framing rate is set to 1000 frame per second, shutter speed is 1/1000s, and resolution is (1024x1024). In the latter technique, a z-type Schlieren imaging setup has been used for tracking droplet combustion as shown in Figure 2. In this setup, a Dolan-Jenner MI-150 fibre optic high intensity illuminator (1) has been used as a light source, and attached to it is a Trixes 40x 25mm magnifier lens (2) for light focus. The droplet setup (4) is aligned between two 12 inch diameter, 10 feet focal length parabolic mirrors (3) which are used for reflecting the light into the high speed camera (9). Attached to the camera is a Nikon AF NIKKOR 50mm f/1.8D lens (7) and the 55mm macro extension tube (8) for magnifying the droplet image. A knife edge (5) has been used for creating the Schlieren effect and a Hoya 49mm close up lens (6) is used for focusing the light towards the camera. Imaging has been carried out at 10000 frames per second to provide sufficient time for tracking, whereas shutter speed and resolution are fixed to 1/10000s and 1024x1024 respectively. The droplet is suspended on the

centre of the SiC fibre mesh. Droplet ignition is performed by heating one of the mesh sides using a butane flame that is placed below the fibre at relatively far distance from the droplet so that no interference between the droplet and flame is taking place. The butane flame is then removed once ignition takes place. Droplet lifetime is evaluated by the appearance and disappearance of the visible flame. The image before the first appearance of the visible flame is assumed as the start of droplet lifetime (t_0), and the image at which the visible flame disappears is assumed as the end of droplet lifetime (t_{total}). Droplet diameter at that former image is assumed as the initial diameter (D_0). The images are recorded for the time between droplet ignition and flame extinction. The acquired images have been stored in (TIFF) format and processed by specifically written algorithms using Matlab. Each test has been repeated four times, from which the average droplet initial diameter is evaluated to be 1.2±0.07 mm.

IMAGE PROCESSING

Matlab has been implemented for processing the images and extracting the required features. A series of processes are performed sequentially on the images to extract the required features. These processes are carried out according to a special algorithm whose sequence is shown in Figure 3. Once read, the image is cropped into a specific size decided by the nature of analysis, whether it is droplet or flame analysis. Then, image enhancement is carried out first by transforming the image from an RGB format into a grayscale format. Then, image complementation is applied in the case of droplet analysis rather than flame analysis, because droplets are shown to be relatively dark in both backlit and shadowgraph imaging techniques. This is due to the droplet being between the light source and camera. Whereas, the flame is luminous by its own and its light intensity is higher than that of the light source, therefore it does

not have the dark appearance of the droplet. Thereafter, hole filling, intensity thresholding, filtering, and opening are applied on the image to isolate the selected object (droplet or flame) for feature extraction. A sample of image processing on diesel fuel droplet is shown in Figure 4. The maximum discrepancy between the extracted object size using the described image processing algorithm and its size on the raw image is 1 pixel. This has resulted in an uncertainty of 0.3% in the results. Morphological operators are then applied on the resulting image for evaluating the area, perimeter, centroid, in the case of droplet, and boundaries length in the case of flame.

RESULTS AND DISCUSSION

Backlit Imaging

Droplet combustion characteristics have been investigated for the diesel/biodiesel blends (BD07, BD10, BD20, and BD30) in addition to those of neat diesel (D100) and neat biodiesel (B100). Backlighting imaging has been used for studying droplet size evolution and the corresponding visible flame dimensions. This technique offers the benefits of sharply visualizing the boundaries of both the droplet and the corresponding flame. These boundaries are then used for tracking and calculating droplet size evolution and flame size variation in response to droplet combustion advancement.

Figure 5(a) shows the sequence of events of BD07 droplet combustion captured by backlighting imaging with each frame representing (1ms) of droplet lifetime. The figure shows that the droplet is relatively circular in shape and its boundaries are highly defined. The flame boundaries and evaporation zone are also well-defined. Figure 5(b) shows the occurrence and development of nucleation inside the droplet. As mentioned earlier, the tests have been repeated

four times for every fuel. The repeatability of droplet burning rate has been measured by evaluating the standard deviation of the resulting droplet burning rate. The standard deviation for D100, B100, and BD10 is evaluated to be 0.05, 0.04, and 0.08 respectively, and for the other fuels is 0.03. These low values of the standard deviation are suggesting a relatively high repeatability of the calculated results.

Figure 6 shows the droplet size evolution for diesel, biodiesel, and diesel/biodiesel blends with time. Droplet size evolution has been estimated using the equivalent circular area of the droplet projected area evaluated by image processing using Matlab. Droplet size evolution is expressed in terms of the normalized droplet diameter square. Droplet diameter is normalized with respect to its initial diameter. This is according to the D^2-law of droplet combustion which states that $(D/D_0)^2=1-K(t/D_0^2)$ [21]. Hence the droplet lifetime has also been divided by the droplet initial diameter squared. From the figure it can be seen that the lifetime of the biodiesel droplet is slightly higher than that of the diesel droplet. And that the lifetime of the blends is proportional with biodiesel concentration in the blend. This suggests that blending biodiesel with diesel leads to enhanced combustion rate and in turn increased fuel consumption. This is in agreement with previous findings on engine performance [8–10]. Additionally, it can be seen that droplet size fluctuation in the diesel/biodiesel blends is higher than that in the base diesel and biodiesel droplets. This is because of the occurrence of secondary atomization from the multicomponent compared to the single-component fuel droplets. The secondary atomization from droplet surface makes it to sustain irregularities in shape as a reaction to the ejection of sub-droplets. This in turn, will result in a wavy shape all around the surface giving the fluctuation in droplet size. Moreover, as shown in the regions highlighted by the circles in Figure 6, for a short time period within the interval bounded by 0.5 and 0.6 s/mm^2 of droplet lifetime, a slightly

constant droplet size pattern is noticed for the blends compared to diesel and biodiesel. This is referred to the heating and evaporation of the less volatile component in the multicomponent mixtures [22]. These components last to the end inside the droplet, and then start to boil and evaporate causing the droplet size to increase due to increased internal pressure by vapour generation [23]. In the present work, biodiesel is the less volatile component [24]. Hence, diesel will evaporate first leaving the biodiesel to accumulate in the centre of the droplet. This will result in a form of nucleation and phase separation between diesel and biodiesel as shown in Figure 5(b). After a certain time, the concentrations of the mixture will change due to diesel depletion and biodiesel accumulation resulting in a new mixture of high biodiesel concentration. Therefore, biodiesel will move towards the droplet surface due to concentration gradient. Though, at the droplet surface, biodiesel will evaporate at a temperature higher than that of diesel. This will result in increasing the droplet surface temperature, and accordingly increasing the temperature inside the droplet. Consequently, the remaining diesel that is trapped inside that droplet will start boiling and generate vapour that will increase the internal pressure of the droplet and causes its expansion. This expansion is shown to occur in the second half of its lifetime and for the diesel and blends rather than biodiesel. For diesel, the expansion is less intensive compared to the diesel/biodiesel blends, and it may be related to constituents of diesel. Since the diesel fuel is a mixture of different components that have different volatilities, making the diesel droplet to behave similarly like the multicomponent fuel droplets. The expansion onset time and occurrence intervals have been evaluated for all the blends and shown in Figure 7. It can be inferred from the figure that the higher the biodiesel content in the mixture the earlier the droplet expansion to occur. However, the overall expansion interval is decreased by increasing biodiesel in the blend. This means that increasing biodiesel in the blend leads to faster

occurrence and faster termination of droplet expansion. This could be linked to the same phase separation process discussed above. Where, increasing biodiesel content in the blend will decrease the time required for the change in concentrations due to diesel depletion and biodiesel accumulation, and therefore, decreasing the expansion onset time. Additionally, increasing biodiesel content in the blend will lead to decreasing diesel concentrations and will reduce the amount of trapped diesel in the droplet centre, and in turn reduces vapour generation rate, leading to the decline in droplet expansion time.

Figure 8 shows the rate of change of droplet size with time for all the investigated fuels. This rate of change is normalized with respect to droplet initial diameter to eliminate the effect of size change between the studied droplets. The negative values illustrate the droplet size reduction, while droplet expansion is shown by the positive values. The figure shows that droplet size fluctuation is higher for the blends when compared to neat diesel and neat biodiesel droplets due to the same reasons mentioned earlier for droplet expansion as a result of volatility difference between diesel and biodiesel. Furthermore, it can be seen from the figure that all the droplets show a slight increase in size in the first 10-20% of the overall droplet lifetime. This is due to the transient heating of the droplet during combustion [25,26].

Figure 9 shows the calculated average burning rate constant of diesel, biodiesel, and their blends respectively. The burning rate constant is the ratio of the droplet initial diameter squared to the droplet lifetime, and it represents the slop of the D^2-t curves shown in Figure 6. Thus, it gives an indication of the burning rate of the fuels under investigation. The figure shows that the burning rate of biodiesel fuel droplet is higher than that of the diesel droplet. This is in agreement with what is found by Li et al., [17] and contradicts the findings of Botero et al., [14]. In addition to the agreement with published data on break specific fuel consumption of the engines fuelled

by diesel biodiesel [27]. This higher burning rate tendency is related to the increase in evaporation rate of biodiesel compared to diesel [17]. Figure 9 shows also that the burning rate of the blends is initially lower than that of diesel, and that increasing biodiesel content in the blends increases the burning rate of the droplet. This is attributed to the higher burning rate of biodiesel compared to diesel, and to the chaotic nature of multicomponent fuel droplet combustion compared to single component diesel.

Figure 10 shows the variation of the luminous flame height with time for diesel, biodiesel, diesel/biodiesel blends of 7, 10, 20, and 30% biodiesel volume in the blend. Flame height has been normalized according to the initial droplet diameter for each fuel. Time as well has been normalized in accordance to the total time required for complete combustion of the droplet, in order to study flame behaviour for all the fuels across the portion of time. From the figure it can be seen that diesel droplet has the highest flame while biodiesel has the lowest, and in between are the flames of the diesel/biodiesel blends. This is attributed to the sooting tendency of the fuels, where biodiesel has a lower sooting tendency compared to diesel that is classified as a sooting fuel. Again, this supports the previous findings of the effect of biodiesel on decreasing soot generation when added to diesel [14–16]. This in fact is the idea behind adding biodiesel to diesel. It can be seen from the figure as well that at the early 10-20% of the overall droplet combustion, there is a dramatic increase in flame height of almost all the fuels except biodiesel. This is due to the combustion of the fuel vapour that is generated by droplet heating and evaporation before ignition. After the vapour is consumed by combustion, flame height decreases to a certain level that is defined by fuel evaporation from the droplet surface and the tendency of this fuel to generate soot during combustion. However, this sudden increase in flame height has not been seen for biodiesel droplet, which could be attributed to the flash point of biodiesel that

is much higher than that of diesel. This means that biodiesel needs a higher temperature for evaporation and ignition, in addition to the aforementioned low sooting tendency of biodiesel. All these factors led to biodiesel flame height being less than that of diesel and diesel/biodiesel blends.

Figure 11 shows the normalized luminous flame width versus normalized combustion time for the droplet combustion of the fuels under investigation. It can be seen from the figure that the diesel flame is the widest among all, followed by the blends, and then it comes the biodiesel flame. Generally, the arrangement is similar to that of Figure 10, except that sudden rise in flame height which is not seen in the width, since vapour is flowing upward. Since flame width is constant and is not affected by buoyancy, then it might be considered as the flame diameter. Especially, when compared with flame results under zero gravity conditions, it shows a good similarity in shape and magnitude [28].

Figure 12 shows the variation of flame height to width ratio with time for the fuels under study. Since the experiments have been carried out in normal gravity, buoyancy will affect flame shape and deviate it from sphericity. Therefore, it is useful to evaluate the ratio of flame height to width with droplet lifetime. The figure shows that the flame height to width ratio for the blends is higher than those of diesel and biodiesel. Since diesel flame width is relatively higher than others due to its higher tendency for soot generation. While biodiesel flame height is relatively lower than others and its flame width is relatively low. This resulted in the flame height to width ratio for both is lower than their blends. Additionally, the figure shows three distinct regions of the ratio with respect to droplet lifetime for almost all the fuels under investigation. The first region is shown in the early 20% of the droplet lifetime, where flame height is relatively large due to increased evaporation rate by initial heating; therefore a large amount of fuel vapour is

accumulated and burned creating a relatively high luminous flame zone. In this region the flame height to width ratio is in the range of 2.5-3.5 for all the studied fuels except biodiesel that has a ratio of 2. The second region is for the next 60% of droplet lifetime, where steady burning of fuel takes place, giving the ratio its major shape and magnitude in the range of 2-2.5 for the blends and 1.5-2 for diesel and biodiesel. The third region is the last 20% of the droplet lifetime, where the flame starts to shrink height wise while its width remains almost the same until the final stages of combustion. These regions are observable in the cases of diesel D100 and the blends BD07, BD10, BD20, and BD30, whereas for biodiesel B100 the first and second regions are almost similar in peaks, with the first region termination is within 15% of droplet lifetime.

Schlieren Imaging

Schlieren imaging gave the possibility of tracking sub-droplet emission by secondary atomization. Therefore, it has been used for tracking and counting the number of sub-droplets emitted for diesel, biodiesel, 7%, 10%, 20%, and 30% diesel/biodiesel blends.

Figure 13 shows the sequence of events for sub-droplet emission from the BD07 droplet. The time difference between images is (100 μs). The sub-droplet had its own flame surrounding it, therefore its detection by Schlieren imaging was easily conceivable.

Figure 14(a) shows the normalized occurrence time of secondary atomization for each fuel averaged for three test samples. The index number refers to the count of secondary atomization occurrence, where 1 refers to the first secondary atomization, and 2 refers to the second and so on. It can be seen from the figure that biodiesel fuel droplet did not experience any secondary atomization during all the tests carried out. The other fuels – including diesel – have experienced secondary atomization from the early stages after ignition (the first 10% in the case of D100,

BD07, and BD30, and the first 20% in the case of BD10 and BD20). It can be seen also that no sub-droplet emission takes place beyond the third quarter of droplet lifetime for all the fuels. This may be attributed to the depletion of the high volatile components in the fuels and the resulting domination of the low volatile components. The combustion of these components - that represent some of the constituents in the case of neat diesel, in addition to biodiesel in the case of blends – will be relatively similar to the combustion of single component fuels. Additionally, it can be seen that at the second half of droplet lifetime of the BD10 and BD20 fuels, a higher time period is separating between each two sub-droplets emission events. Moreover, droplet secondary atomization could be a random process; therefore qualitative investigation of the process is required. Hence the repeatability of secondary atomization has been estimated for each of the studied fuels by testing it three times. The average and maximum value of the standard deviation evaluated for secondary atomization occurrence along the droplet lifetime for all the studied fuels is shown in Figure 14(b). The figure shows that the standard deviation is relatively low implying a good repeatability of results. This suggests that secondary atomization is not a random process and that it follows a certain trend along the droplet lifetime.

Figure 15 shows the effect of biodiesel concentration on the rate of secondary atomization from the burning droplet of diesel/biodiesel blends expressed in terms of the average sub-droplet emission time. The results represent the average of three tests for each fuel. The emission time is normalized by the initial droplet diameter squared for each fuel. The sub-droplets emission time refers to the interval of time between two successful emissions. That is the higher the time, the lower the fuel tendency for secondary atomization. Hence, it can be seen from the figure that the sub-droplets emission time of the blends is higher than that of diesel. Though, increasing biodiesel concentration in the blend decreases the emission time, which in turn, implies an

enhanced atomization tendency. However, the BD07 emission time values are shown to be closer to those of diesel rather than the BD10.

CONCLUSIONS

In the present work an experimental investigation for the droplet combustion of diesel, biodiesel, and diesel/biodiesel blends of 7%, 10%, 20%, and 30% biodiesel concentration has been carried out. The followings have been found:

- The burning rate constant of the biodiesel droplet is higher than that of the diesel droplet. And that the lifetime of the blends is proportional to biodiesel concentration in the blend. This suggests that blending biodiesel with diesel leads to enhanced combustion rate and in turn increased fuel consumption. This is in agreement with previous findings on engine performance.
- Droplet size fluctuation in the diesel/biodiesel blends is higher than that in the base diesel and biodiesel droplets. This is because of the occurrence of secondary atomization from the multicomponent droplets compared to the single-component droplet. The biodiesel-blended diesel droplets have shown a slight freezing in size because of the heating and evaporation of biodiesel. Biodiesel lasts to the end inside the droplet, and then start to boil and evaporate causing the droplet size to increase due to increased internal pressure by vapour generation.
- Droplet expansion is shown to occur in the second half of its lifetime and for the diesel and blends rather than biodiesel. For diesel, the expansion is less intensive compared to the diesel/biodiesel blends, and it may be related to the constituents of the diesel. The higher the biodiesel content in the mixture the earlier the droplet expansion to occur. However, the overall expansion interval is decreased by increasing biodiesel in the blend.

- The burning rate of diesel fuel droplet is marginally higher than that of biodiesel droplet. The marginal difference between diesel and biodiesel droplets burning rate is attributed to the difference in physical properties. And that increasing biodiesel content in the blends increases the burning rate of the droplet.
- Diesel droplet has the highest flame length while biodiesel has the lowest, and in between are the flames of the diesel/biodiesel blends. This is attributed to the sooting tendency of the fuels, where biodiesel has a lower sooting tendency compared to diesel that is classified as a sooting fuel. At the early 10-20% of the overall droplet combustion, there is a dramatic increase in flame height of almost all the fuels except biodiesel. This is due to the combustion of the fuel vapour that is generated by droplet heating and evaporation before ignition. However, this sudden increase in flame height has not been seen for biodiesel droplet, which could be attributed to the flash point of biodiesel that is much higher than that of diesel, in addition to the low sooting tendency of biodiesel.
- Schlieren imaging gave the possibility of tracking sub-droplet emission by secondary atomization. Therefore, it has been used for tracking and counting the number of sub-droplets emitted for all the fuels.
- Biodiesel fuel droplet did not experience any secondary atomization during all the tests carried out. The other fuels – including diesel – have experienced secondary atomization from the early stages after ignition (the first 10% in the case of D100, BD07, and BD30, and the first 20% in the case of BD10 and BD20).
- No sub-droplet emission takes place beyond the third quarter of droplet lifetime for all the fuels. This may be attributed to the depletion of the high volatile components in the fuels and

the resulting domination of the low volatile components. The combustion of these components will be relatively similar to the combustion of single component fuels.

- The secondary atomization is not a random process and that it follows a certain trend along the droplet lifetime. Sub-droplets emission time of the blends is higher than that of diesel. Though, increasing biodiesel concentration in the blend decreases the emission time, which in turn, implies an enhanced atomization tendency.

NOMENCLATURE

D	[mm]	Droplet diameter
K	[mm^2/s]	Burning rate constant
H	[mm]	Flame height
t	[s]	Time
W	[mm]	Flame width

Subscripts

i	[-]	Instantaneous
0	[-]	Initial
total	[-]	Total time

Fuels

B100	Neat Biodiesel
BD07	93%Diesel+7% Biodiesel
BD10	90%Diesel+10% Biodiesel
BD20	80%Diesel+20% Biodiesel
BD30	70%Diesel+30% Biodiesel
D100	Neat Diesel

ACKNOWLEDGMENTS

The work is partly sponsored by the Newton Research Collaboration Programme of Royal Academy of Engineering. Additionally, the authors would like to thank each of: HCED (Iraq), EPSRC (United Kingdom), FAPEMIG and CNPq (Brazil) for their supports to each of the authors respectively.

REFERENCES

[1] Zhu, L., Cheung, C. S., Zhang, W. G., Huang, Z. Combustion, performance and emission characteristics of a DI diesel engine fueled with ethanol-biodiesel blends, *Fuel*, vol. 90, pp. 1743–1750, 2011.

[2] Candeia, R. A., Silva, M. C. D., Carvalho Filho, J. R., Brasilino, M. G. A., Bicudo, T. C., Santos, I. M. G., Souza, A.G. Influence of soybean biodiesel content on basic properties of biodiesel-diesel blends, *Fuel*, vol. 88, pp. 738–743, 2009.

[3] Benjumea, P., Agudelo, J., Agudelo, A. Basic properties of palm oil biodiesel-diesel blends, *Fuel*, vol. 87, pp. 2069–2075, 2008.

[4] Pucher, G., Allan, W., LaViolette, M., Poitras, P. Emissions from a gas turbine sector rig operated with synthetic aviation and biodiesel fuel, *Journal of Engineering for Gas Turbines and Power*, vol. 133, pp. 111502(1-8), 2011.

[5] Chiaramonti, D., Rizzo, A. M., Spadi, A., Prussi, M., Riccio, G., Martelli, F. Exhaust emissions from liquid fuel micro gas turbine fed with diesel oil, biodiesel and vegetable oil, *Applied Energy*, vol. 101, pp. 349–356, 2013.

[6] Kurji, H., Valera-Medina, A., Runyon, J., Giles, A., Pugh, D., Marsh, R., Cerone, N., Zimbardi, F., Valerio, V. Combustion characteristics of biodiesel saturated with pyrolysis oil for power generation in gas turbines, *Renewable Energy*, vol. 99, pp. 443–451, 2016.

[7] Kushwah, Y.S., Mahanta, P., Mishra, S.C. "Some studies on fuel characteristics of mesua ferrea, *Heat Transfer Engineering*, vol. 29, pp. 405–409, 2008.

[8] Habibullah, M., Masjuki, H. H., Kalam, M. A., Rizwanul Fattah, I. M., Ashraful, A. M., Mobarak, H.M. Biodiesel production and performance evaluation of coconut, palm and their combined blend with diesel in a single-cylinder diesel engine, *Energy Conversion*

and Management, vol. 87, pp. 250–257, 2014.

[9] Yasin, M. H. M., Paruka, P., Mamat, R., Yusop, A. F., Najafi, G., Alias, A. Effect of low proportion palm biodiesel blend on performance, combustion and emission characteristics of a diesel engine, *Energy Procedia*, vol. 75, pp. 92–98, 2015.

[10] Ileri, E., Atmanli, A., Yilmaz, N. Comparative analyses of n-butanole-rapeseed oil-diesel blend with biodiesel, diesel and biodiesel-diesel fuels in a turbocharged direct injection diesel engine, *Journal of the Energy Institute*, vol. 89, pp. 586–593, 2016.

[11] Zhang, Y., Huang, R., Wang, Z., Xu, S., Huang, S., Ma, Y. Experimental study on puffing characteristics of biodiesel-butanol droplet, *Fuel*, vol. 191, pp. 454–462, 2017.

[12] Rahman, S. M. A., Masjuki, H. H., Kalam, M. A., Abedin, M. J., Sanjid, A., Sajjad, H. Production of palm and calophyllum inophyllum based biodiesel and investigation of blend performance and exhaust emission in an unmodified diesel engine at high idling conditions, *Energy Conversion and Management*, vol. 76, pp. 362–367, 2013.

[13] Mukhopadhyay, A., Sanyal, D. Modeling of evaporation and combustion of droplets in a spray using the unit cell approach: a review, *Heat Transfer Engineering*, vol. 33, pp. 375–386, 2012.

[14] Botero, M. L., Huang, Y., Zhu, D. L., Molina, A., Law, C.K. Synergistic combustion of droplets of ethanol, diesel and biodiesel mixtures, *Fuel*, vol. 94, pp. 342–347, 2012.

[15] Pan, K. L., Li, J. W., Chen, C. P., Wang, C.H. On droplet combustion of biodiesel fuel mixed with diesel/alkanes in microgravity condition, *Combustion and Flame*, vol. 156, pp. 1926–1936, 2009.

[16] Pan, K. L., Chiu, M.C. Droplet combustion of blended fuels with alcohol and biodiesel/diesel in microgravity condition, *Fuel*, vol. 113, pp. 757–765, 2013.

[17] Li, T. X., Zhu, D. L., Akafuah, N. K., Saito, K., Law, C.K. Synthesis, droplet combustion, and sooting characteristics of biodiesel produced from waste vegetable oils, *Proceedings of the Combustion Institute*, vol. 33, pp. 2039–2046, 2011.

[18] Zhu, M., Ma, Y., Zhang, Z., Chan, Y. L., Zhang, D. Effect of oxygenates addition on the flame characteristics and soot formation during combustion of single droplets of a petroleum diesel in air, *Fuel*, vol. 150, pp. 88–95, 2015.

[19] Xu, Y., Keresztes, I., Condo, A. M., Phillips, D., Pepiot, P., Avedisian, C.T. Droplet combustion characteristics of algae-derived renewable diesel, conventional #2 diesel, and their mixtures, *Fuel*, vol. 167, pp. 295–305, 2016.

[20] Wang, Z.G. Internal Combustion Processes of Liquid Rocket Engines: Modeling and Numerical Simulations, *John Wiley and Sons Ltd.*, 2016.

[21] Turns, S.R. An Introduction To Combustion - Concepts and Applications." 3rd edition, *McGraw-Hill*, 2012.

[22] Wang, C. H., Liu, X. Q., Law, C.K. Combustion and microexplosion of freely falling multicomponent droplets, *Combustion and Flame*, vol. 56, pp. 175–197, 1984.

[23] Lasheras, J. C., Fernandez-Pello, A. C., Dryer, F.L. On the disruptive burning of free droplets of alcohol/n-paraffin solutions and emulsions, *Symposium (International) on Combustion/The Combustion Institute*, vol. 18, pp. 293–305, 1981.

[24] Kalogeras, K., Bezergianni, S., Kazantzi, V., Pilavachi, P.A. On the prediction of properties for diesel/biodiesel mixtures featuring new environmental considerations, *Computer Aided Chemical Engineering*, vol. 28, pp. 973–978, 2010.

[25] Law, C.K. Unsteady droplet combustion with droplet heating, *Combustion and Flame*, vol. 26, pp. 17–22, 1976.

[26] Law, C. K., Sirignano, W.A. Unsteady droplet combustion with droplet heating-II: conduction limit, *Combustion and Flame*, vol. 28, 175–186, 1977.

[27] Lešnik, L., Vajda, B., Žunič, Z., Škerget, L., Kegl, B. The influence of biodiesel fuel on injection characteristics, diesel engine performance, and emission formation, *Applied Energy*, vol. 111, pp. 558–570, 2013.

[28] Liu, Y. C., Farouk, T., Savas, A. J., Dryer, F. L., Avedisian, C.T. "On the spherically symmetrical combustion of methyl decanoate droplets and comparisons with detailed numerical modeling, *Combustion and Flame*, vol. 160, pp. 641–655, 2013.

Table 1: Diesel and biodiesel properties

Fuel Property	Unit	Diesel	Biodiesel
Kinematic Viscosity @ 40ºC	mm^2/s	3.05[(a)]	4.363[(a)]
Density @ 15.5	kg/m^3	830[(a)]	877.8[(a)]
Specific Gravity @ 15.5	---	0.83[(a)]	0.88[(a)]
Flash Point	ºC	79[(a)]	122[(a)]
Cloud Point	ºC	3[(a)]	5[(a)]
Boiling Point	ºC	181[(b)]	302[(b)]
Pour Point	ºC	-35 to -15[(b)]	-15 to 10[(b)]
Higher Heating Value	MJ/kg	47.8[(b)]	41.2[(b)]
Lower Heating Value	MJ/kg	43.2[(b)]	37.1[(b)]
Latent Heat of Vaporization	kJ/kg	254[(b)]	254[(b)]
(a) From the supplier.		(b) From literature.	

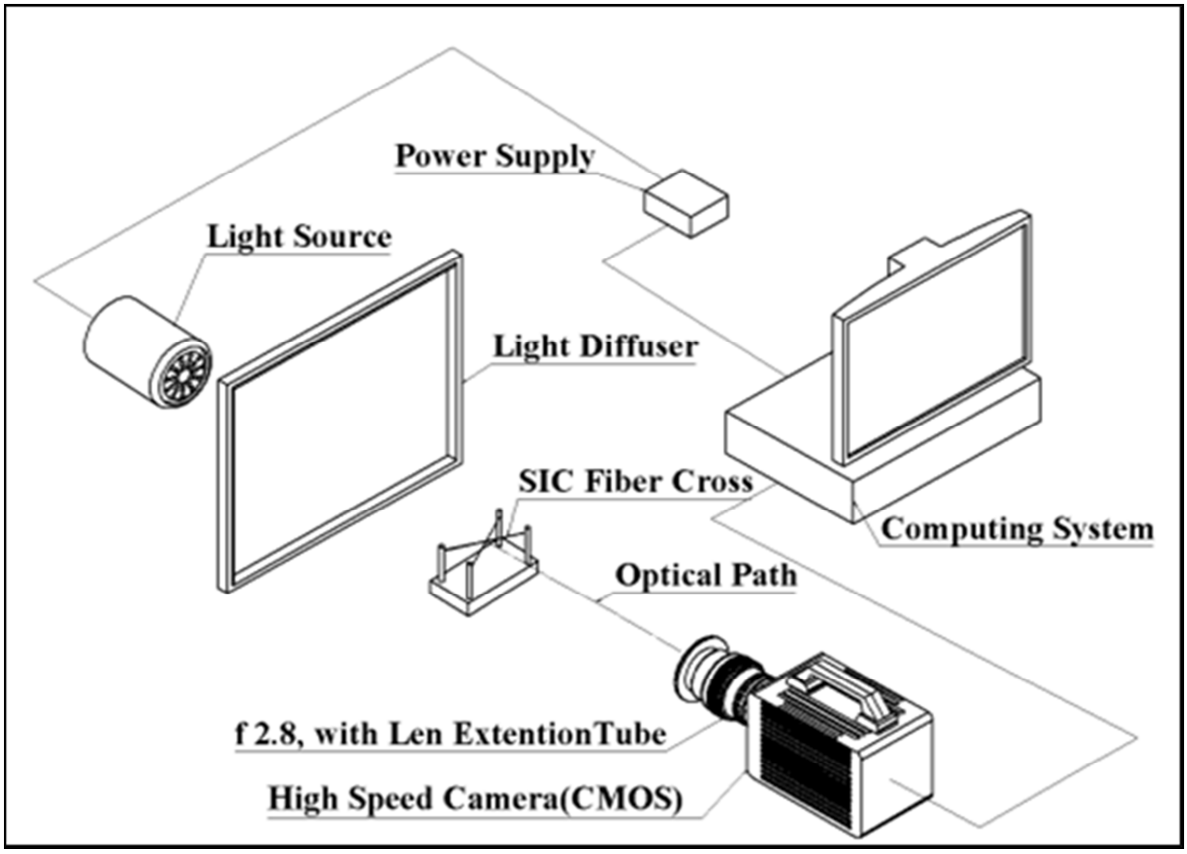

Figure 1 Backlit imaging setup.

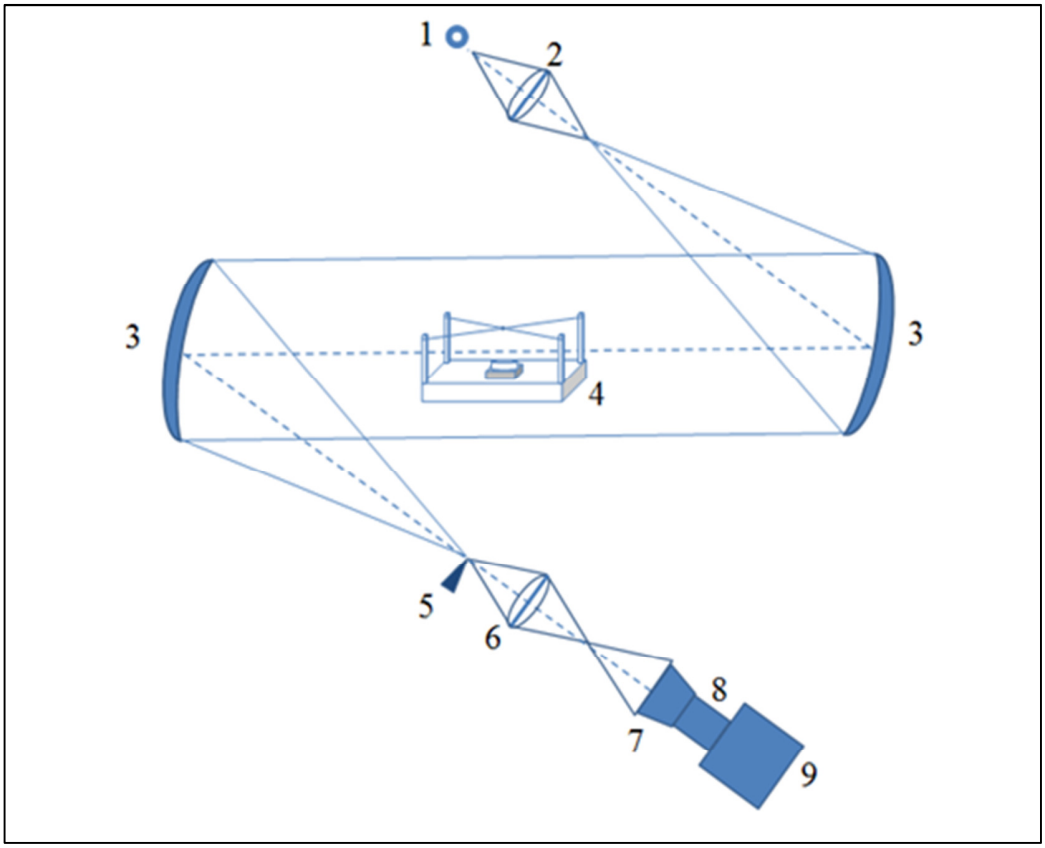

Figure 2 Schlieren imaging setup.

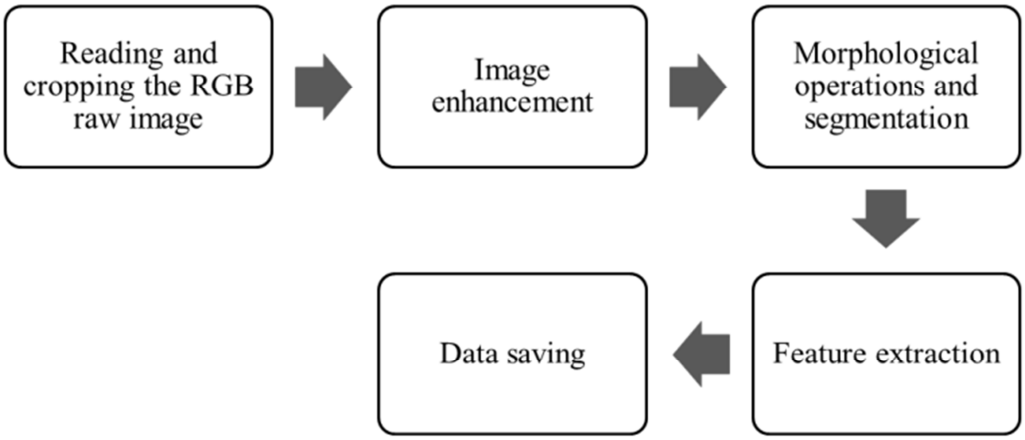

Figure 3 Image processing flowchart.

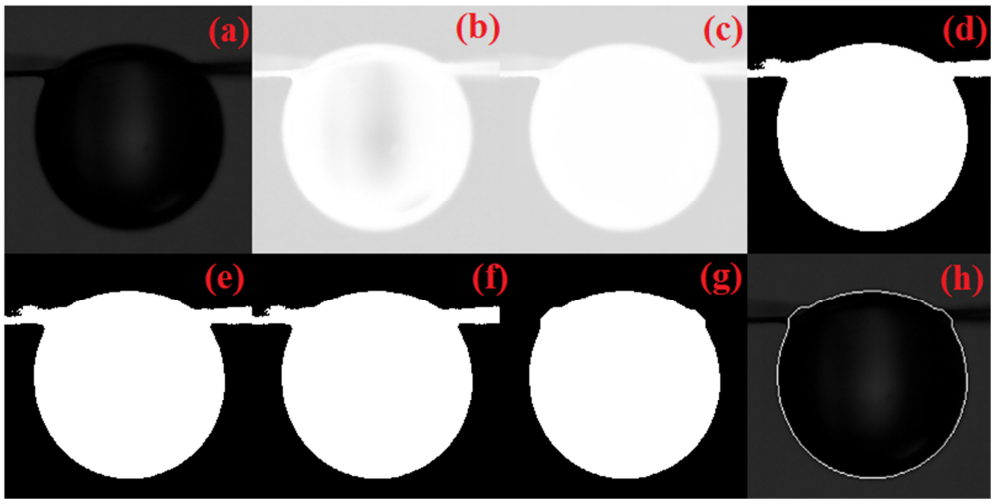

Figure 4 Sequence of image processing to isolate biodiesel droplet from its surroundings; (a) the cropped grayscale image, (b) complementation, (c) holes filling (first), (d) thresholding, (e) noise removal by filtering, (f) holes filling (second), (g) final imge of the isolated droplet, (h) boundaries of (g) matched with (a).

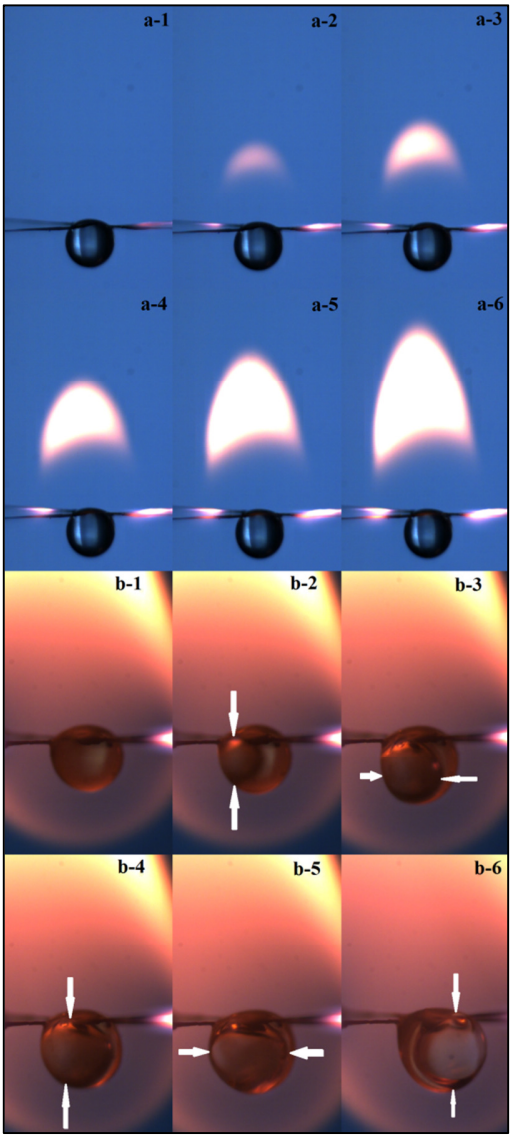

Figure 5 BD07 droplet combustion images showing: (a1-6) droplet and flame, (b1-6) nucleation evolution and development.

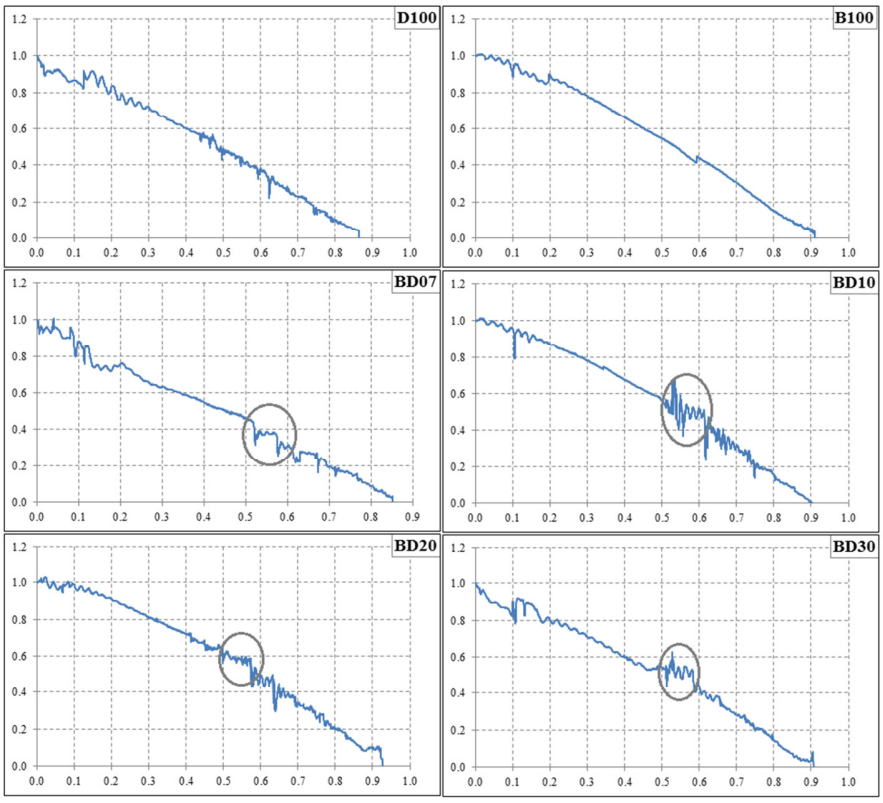

Figure 6 Droplet size evolution with respect to time for all the fuels under investigation; the y-axis is the normalized droplet size $(D/D_0)^2$, and the x-axis is the normalized droplet lifetime $(t/\mathbf{D_0^2})$.

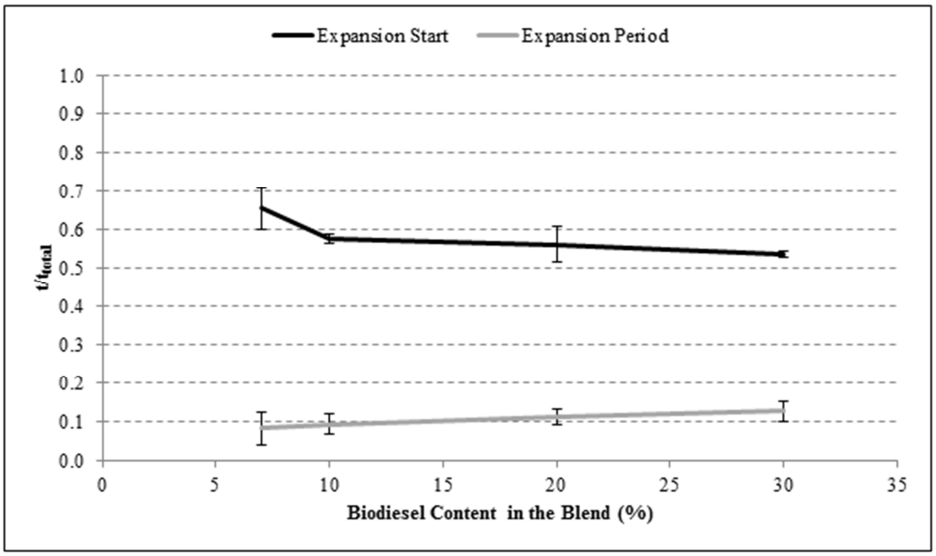

Figure 7 The effect of biodiesel concentration on the droplet expansion starting time and occurrence interval.

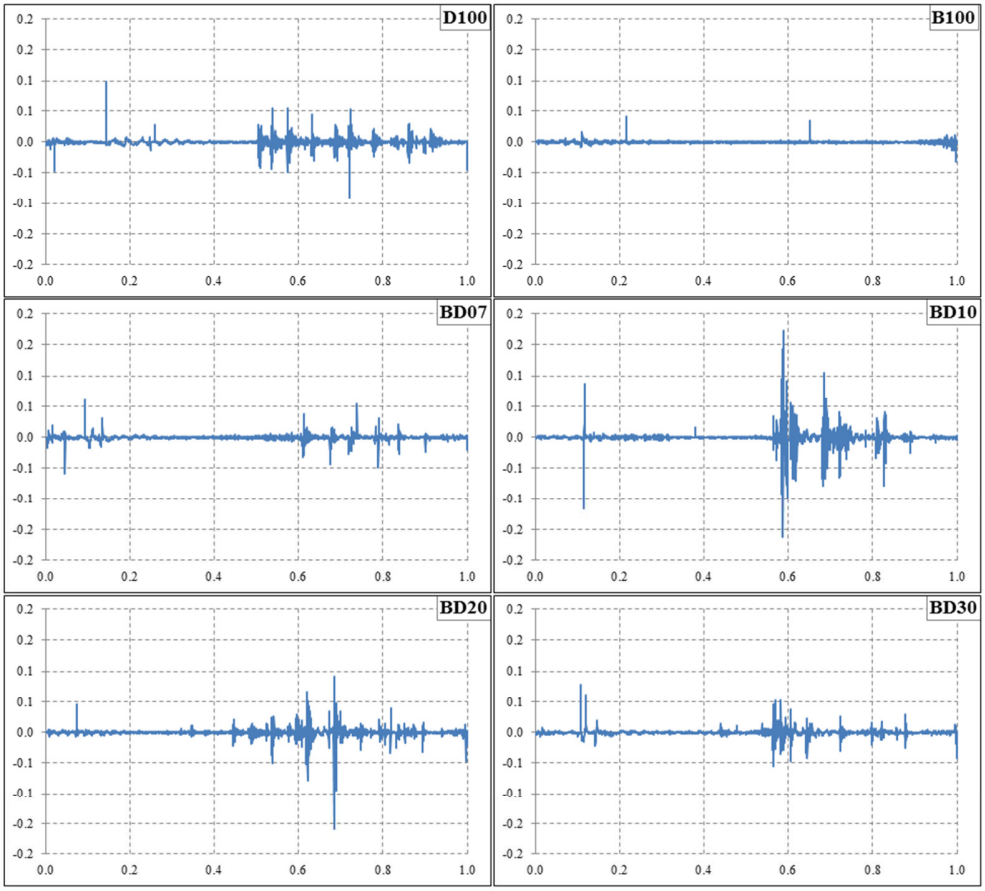

Figure 8 Normalized droplet size fluctuation with respect to the normalized droplet lifetime (t/t_{total}) for the fuels under investigation.

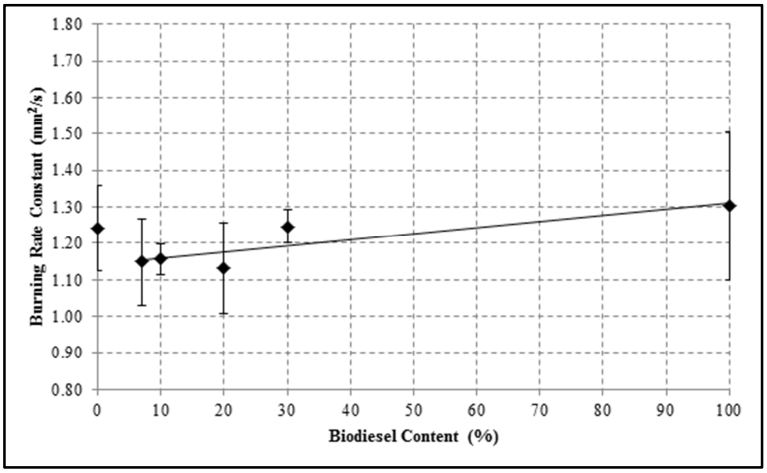

Figure 9 The effect of biodiesel concentration on the burning rate constant.

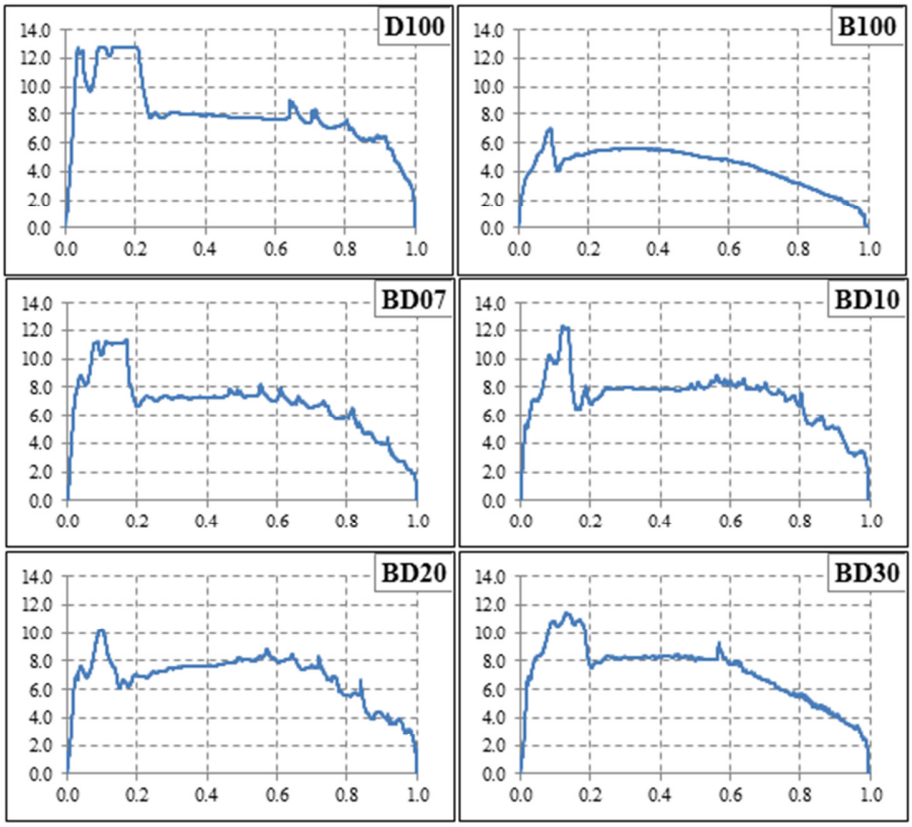

Figure 10 Variation of the normalized flame height (H/D_0) with normalized lifetime (t/t_{total}) for D100, B100, BD07, BD10, BD20, and BD30 droplets.

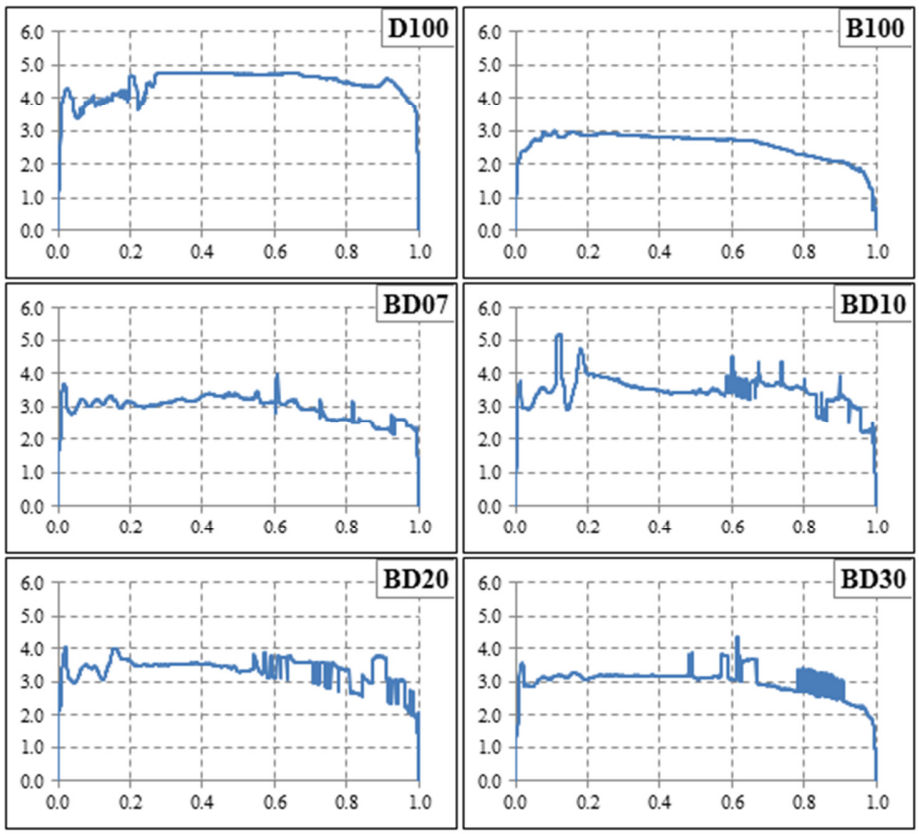

Figure 11 Variation of the normalized flame width (W/D_0) with normalized lifetime (t/t_{total}) for D100, B100, BD07, BD10, BD20, and BD30 droplets.

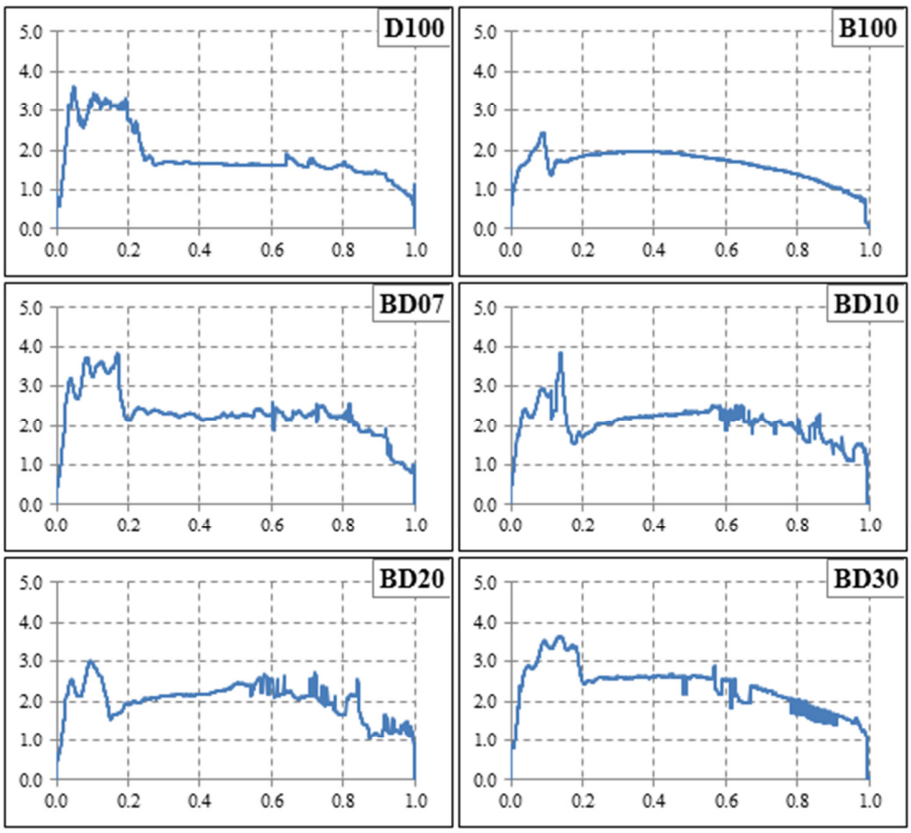

Figure 12 Variation of flame height/width ratio (H/W) with normalized lifetime (t/t_{total}) for D100, B100, BD07, BD10, BD20, and BD30 droplets.

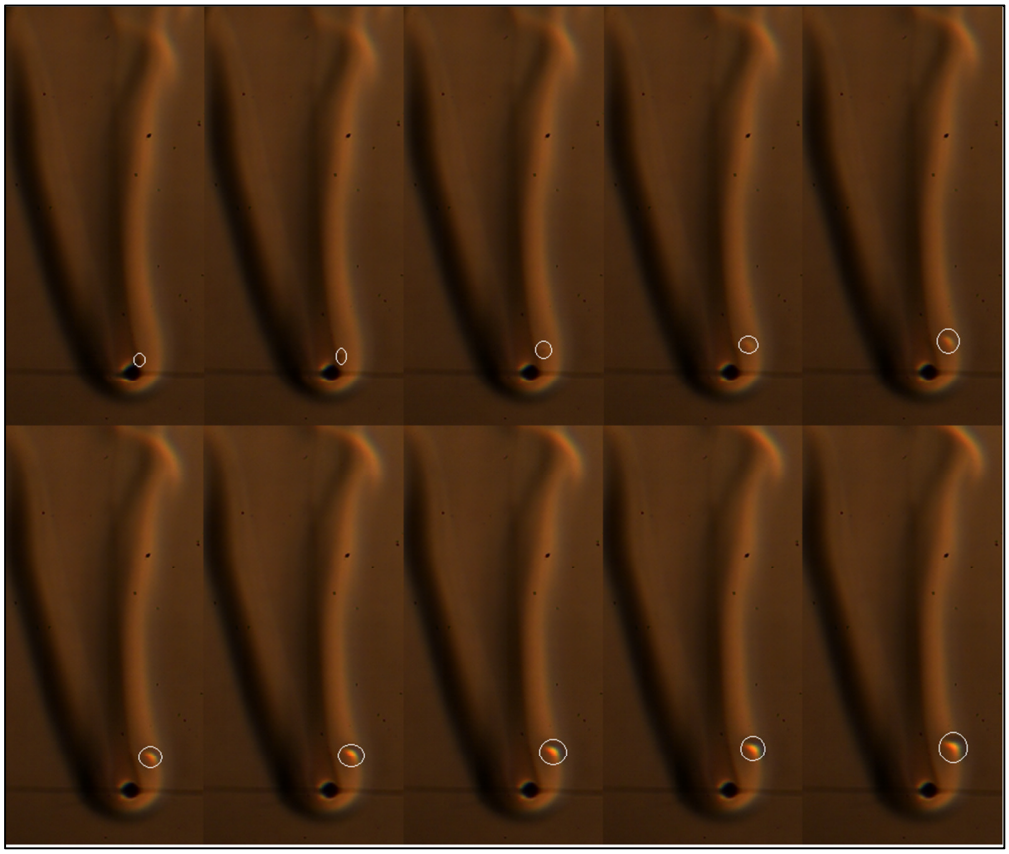

Figure 13 Schlieren images of secondary atomization from a BD07 droplet.

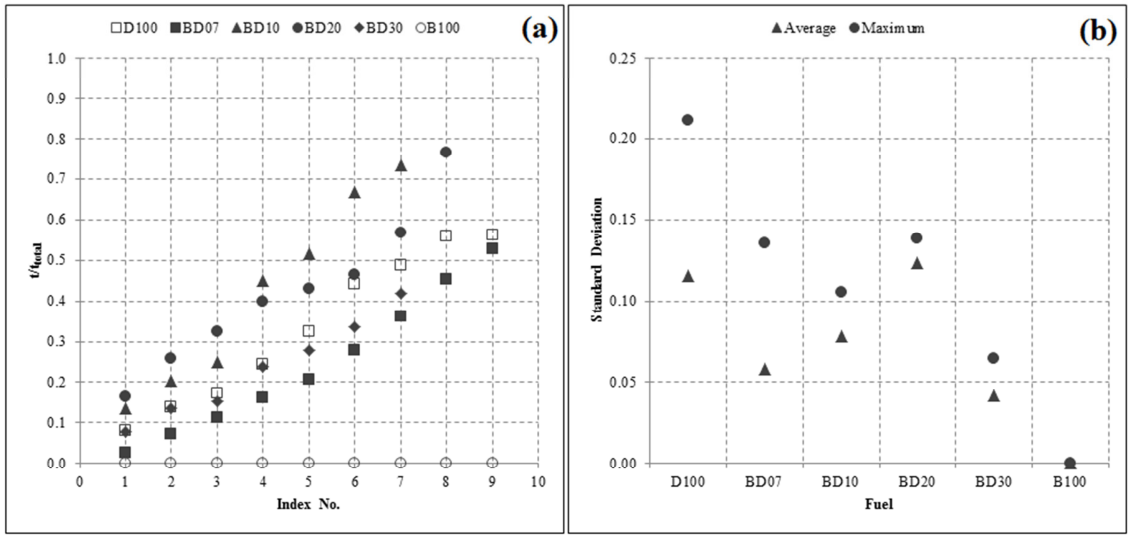

Figure 14 (a) Occurrence time of droplet secondary atomization for diesel, biodiesel, and their blends, (b) average and maximum standard deviation of three tests for each fuel.

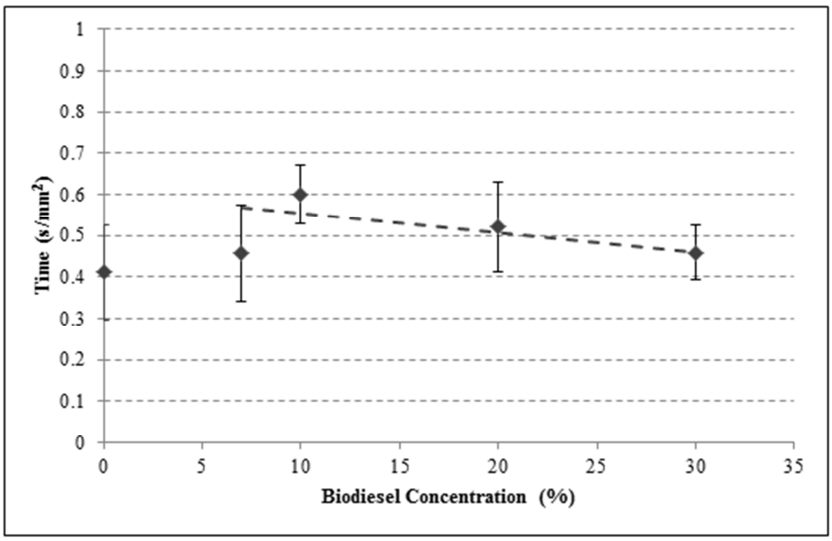

Figure 15 Average sub-droplet emission time with respect to biodiesel concentration in the diesel/biodiesel blend.

List of Figure Captions

Ahmad Muneer El-Deen Faik is a PhD student at the Combustion and Flow Diagnostics Research Group, Mechanical Engineering Department, the University of Sheffield, United Kingdom. He received his B.Sc. and M.Sc. in Mechanical Engineering from Al-Nahrain University, Iraq at 2003 and 2006 respectively. He is currently working on high speed focused imaging of the droplet dynamics during combustion.

Yang Zhang is Professor of combustion and energy in the Mechanical Engineering Department of the University of Sheffield. He received his BEng degree from Zhejiang University, China, and PhD in the Engineering Department of Cambridge University, where he then worked as a Research Associate and a Research Fellow at Darwin College at the same time. Afterwards, he moved to the Manchester University Institute of Science and Technology before taking the Chair of Combustion and Energy in Sheffield. His laboratory specializes in combustion and advanced flow diagnostics using both conventional and in-house developed techniques. He is also the author of many publications in this field.

Sergio Hanriot is Professor of the Post-Graduate Programme in Mechanical Engineering of the Pontifical Catholic University of Minas Gerais, Brazil. He received his PhD in Mechanical Engineering in the area of Thermal and Fluids 2011. Part of the studies has done at the FIAT Research Centre (CRF) in Turin, Italy. His area of research emphasises on internal combustion engines, pulsating flow, applied fluid dynamics, refrigeration, compressible flow and waves. In an administrative position, the following positions were held: Chief and Coordinator of the Department of Mechanical Engineering, Vice-Director of the Polytechnic Institute of PUC-Minas, Pro-Rector of Logistics and Operations, Executive Director of the Mariana Resende Costa Foundation. He currently holds the position of Provost of Research and Post-Graduation Studies.